Science Press

ARTICLE

Effects of Indium Sulfide on the Structure and Corrosion Resistance of the Micro-arc Oxidation Coating on ZL108 Alloy

Wang Ping[1,2,3],   Hu Jie[1],   Li Ruiyang[1],   Gong Zeyu[1],   Liu Jiwei[1],   Xiong Dan[1],
Xiang Dong[1],   Wei Xiaowei[3],   Zu Xiaotao[2]

[1] School of Materials Science and Engineering, Southwest Petroleum University, Chengdu 610500, China; [2] School of Physics, University of Electronic Science and Technology of China, Chengdu 611731, China; [3] School of Materials Science and Engineering, Xihua University, Chengdu 610039, China

Abstract: Micro-arc oxidation (MAO) coatings were formed on ZL108 aluminum alloy in the silicate electrolyte with In_2S_3. Scanning electron microscopy (SEM), optical profilometer, X-ray diffraction (XRD), X-ray photoelectron spectroscopy (XPS) and electrochemical workstation were used to study the effects of In_2S_3 on the micro-structure, phase composition and corrosion resistance of the micro-arc oxidation coating. The results show that the addition of In_2S_3 increased the micro-arc oxidation voltage so the coating formation rate was increased, which resulted in the increasing of the thickness of the micro-arc oxidation coating. The micro-arc oxidation coating formed in the electrolyte containing In_2S_3 had higher density and micro-hardness, resulting in the enhanced corrosion resistance. The phases of the micro-arc oxidation coating were mainly composed of α-Al_2O_3, γ-Al_2O_3 and SiO_2. XPS test result shows that In_2S_3 was converted to In_2O_3 during the micro-arc oxidation process. Therefore, the addition of In_2S_3 can optimize the structure of the micro-arc oxidation coating and improve its comprehensive properties.

Key words: micro-arc oxidation; ZL108 alloy; indium sulfide; corrosion resistance

ZL108 alloy has been increasingly used in piston manufacturing industry, but its low corrosion resistance limits its extensive application. For further applications, various surface treatments have been applied to improve the corrosion resistance[1-3]. As a cost-effective and environment-friendly surface treatment technology, micro-arc oxidation can effectively improve the corrosion resistance[4,5].

Micro-arc oxidation (MAO) is also known as "plasma electrolytic oxidation (PEO)" and it is an effective method for preparing ceramic coatings on light alloys[6,7]. The purpose of MAO technology is to obtain coatings with excellent structure and good corrosion resistance and it has been successfully prepared on Al[8,9], Mg[10,11], Ti[12] and their alloys.

There have been many studies on the corrosion resistance of MAO coatings[13-16]. The results showed that MAO coatings have good corrosion resistance. However, the thickness, micro-hardness and corrosion resistance of MAO coatings can no longer satisfy the more and more severe working conditions. Doping with some special functional dopants can effectively solve these problems[17-19]. In_2S_3 is a kind of dopant with special functions, but the research on it mainly focuses on the optical electrical and structural properties of In_2S_3 thin films[20-22]. There is no study on the structure and corrosion resistance of the MAO coating with In_2S_3. This work mainly investigated the influence of In_2S_3 on the micro-arc oxidation voltage and the coating structure, and finally understood the influence of In_2S_3 on the corrosion resistance of the MAO coating.

1 Experiment

1.1 Materials

ZL108 alloy was used as the substrate, and the main chemical composition of the substrate is 0.4%~0.9% Mn, 0.5%~1.0%Mg, 1.0%~2.0%Cu, 11.0%~13.0%Si and balanced Al. The size was 20 mm×10 mm×2 mm. Before the MAO treatment, the substrate was polished with 600[#], 1000[#], and 1200[#] frosted silicon carbide papers, then cleaned with distilled water and acetone, and dried naturally in air.

1.2 MAO treatment of ZL108 alloy

A pulse DC power supply (DWL20-6) was adopted for the MAO treatment. The frequency was 100 Hz and the oxidation treatment time was 30 min. The ZL108 alloy was attached to the anode. The stainless steel plate was used as the opposite cathode and placed in the electrolyte to form a closed loop with the sample. The constant current density was set as 6 A/dm^2, the duty cycle was 60%, the basic value was 0 V and the temperature of the electrolyte was kept below 30 ºC during the MAO experiment. Samples treated with micro-arc oxidation were washed with distilled water and dried in air. The electrolyte was composed of Na_2SiO_3 (20 g/L), glycerin (2 mL/L) and NaOH (0.2 g/L). The MAO samples in the base electrolyte was denoted as G0. And In_2S_3 was added to the base electrolyte to prepare the modified electrolyte. The MAO sample prepared in modified electrolyte was G1. The basic electrolyte and modified electrolyte were stirred and placed for 24 h before MAO treatment to make the ions in the solution more stable.

1.3 Characterization of the MAO coating

The surface and cross-section morphologies of the coating were observed by the scanning electron microscope (SEM, ZEISS EVO MA15, Germany), the 3D topography was observed by the Optical Profiler (Bruker Contour GT-InMotion GTK-16-0314, America) and the distribution of element on the surface of the MAO coating was determined by the X-ray energy dispersive spectrometer (EDS, OXFORD 20, America). The X-ray diffraction (XRD, DX-2700B, China) was used to analyze the composition of the phase. And the diffraction data was acquired with scattering angle 2θ from 10° to 80°, and scanning speed was 0.04°/s. The chemical states of In in the coating was analyzed by X-ray photoelectron spectroscopy (XPS). The surface micro-hardness was measured by Digital micro-hardness tester (HXD-2000TM/LCD, China) with load of 1 N for 15 s. Fifteen random points were measured on the surface of each sample, and the average value of these points was calculated to represent the micro-hardness of them. The thickness of the coating was measured by Eddy Current Thickness Gauge (TT230, China). Ten points of each coating were tested and the average value was taken as the thickness value of the MAO coating.

1.4 Electrochemical corrosion tests

Electrochemical Workstation (Gamry Reference 3000,

America) was applied to acquire electrochemical impedance spectroscopy (EIS) and polarization curves in 3.5 wt% NaCl solution at room temperature severally. The reference electrode (RE) was saturated calomel electrode, and the auxiliary electrode (CE) was platinum electrode. The surface area of the sample exposed in NaCl solution was 0.5 cm^2. The sample was used as the working electrode and soaked in NaCl solution for 0.5 h to ensure that the solution reached a stable state before each test. The scanning rate of polarization test was 0.1 mV·s^{-1} and the potential range was from -1.8 to -1.2 V according to open circuit potential (OCP) with -1.7 V. EIS test was done in the frequency range of 100 kHz to 0.01 Hz. The experimental data of EIS were fitted by ZSimDemo.

2 Results and Discussion

2.1 Voltage-time curves

The voltage-time curves of MAO coatings formed on ZL108 alloy surface in the electrolyte without (G0) and with (G1) In_2S_3 are shown in Fig. 1. It is evident that the voltage-time curves consisted of two phases. In the first phase, the voltages of the coating G0 and G1 suddenly increased to around 450 V within 7.5 and 5 min. At this stage, the voltage growth rate of G1 exceeded that of G0. In the second stage, the voltage increased slowly and became stable with the increase of micro-arc oxidation time. It can be clearly seen from the figure that in the electrolyte without and with In_2S_3, the termination voltage of micro-arc oxidation reached about 490 and 510 V, respectively. It can be easily concluded that the voltage in the electrolyte with In_2S_3 was higher than that without In_2S_3. The reason for the two different types of voltage-time curves was that the addition of In_2S_3 promoted MAO reaction and increased the growth rate of the MAO coating. In this case, the thickness of the MAO coating was increased, which can increase the resistance of the coating. The voltage increased because the coating resistance increased [23].

2.2 Morphologies and chemical composition of the MAO coating

The surface morphologies of MAO coatings (G0 and G1) formed on ZL108 alloy are illustrated in Fig.2a and 2c. In the process of micro-arc oxidation, many discharge micropores were generated. Numerous micro-arc discharges occurred during the MAO process, and the adjacent discharge micropores fused and became larger, forming the strip micropores as shown in Fig. 2a. Under the quenching action of the surrounding solution, the molten ejected from the discharge channel was rapidly solidified and irregularly accumulated around the discharge micropores. Therefore, the surface porosity of G0 was higher and the coating roughness was larger. The surface morphology of G1 is shown in Fig. 2c. After In_2S_3 was added, the discharge center was formed on the surface of the MAO coating, making the discharge of the MAO coating more uniform. Therefore, compared with G0, the molten on the MAO coating surface decreased, and
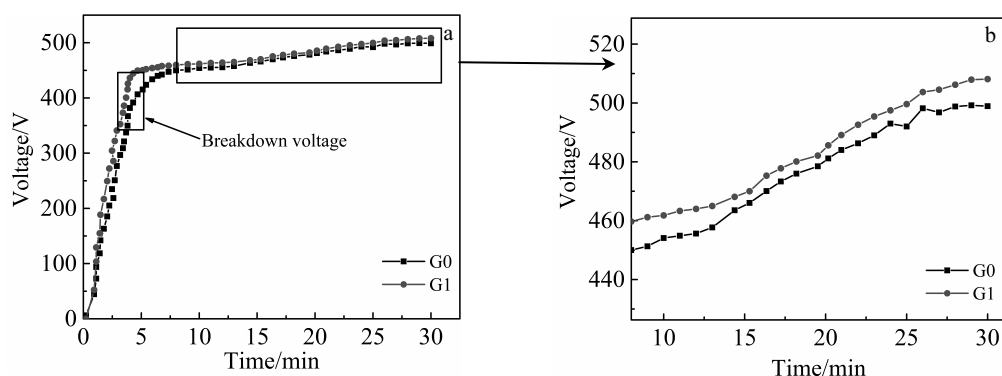
Fig.1   Voltage-time curves for MAO process in electrolytes without (G0) and with (G1) In_2S_3: (a) original drawing and (b) enlarged drawing

the size of the discharge micropores and roughness of the surface decreased. The surface roughness of MAO coatings (G0 and G1) are shown in Fig. 2b and 2d. By comparison, it can be concluded that the fluctuation of the coating after adding In_2S_3 decreased. Moreover, the average roughness of G0 and G1 were 6.164 and 4.946 μm, respectively, which also proved that adding In_2S_3 can smooth the MAO coating. In order to judge the chemical composition of MAO coatings, EDS analysis were performed (shown in Table 1). As can be seen from the change of element content in G0 and G1, during the formation process of MAO coatings, the formation was a result of both the outward migration of Al^{3+} from the ZL108 alloy substrate and the inward migration of O^{2-} and Si^{4+} from the silicate electrolyte. Moreover, it is clearly seen that no In element was

measured in G0, but In element was detected in G1. It is obvious that In element originated from In_2S_3. In summary, it is a feasible, reasonable and promising selection by adding In_2S_3 into the electrolyte to make the surface denser.

By observing the cross-section morphology of the MAO coating in Fig.3, it can be found that the thickness of the coating increased when the In_2S_3 was added, which was consistent with the previous study.

2.3   Phase analysis of the MAO coating

Fig.4a shows the XRD patterns of MAO coatings G0 and G1. The results showed that the phases of MAO coatings were mainly composed of γ-Al_2O_3, α-Al_2O_3 and SiO_2. The main peak of Al can be detected because X-ray can penetrate into the substrate through the MAO coating [24]. The phase
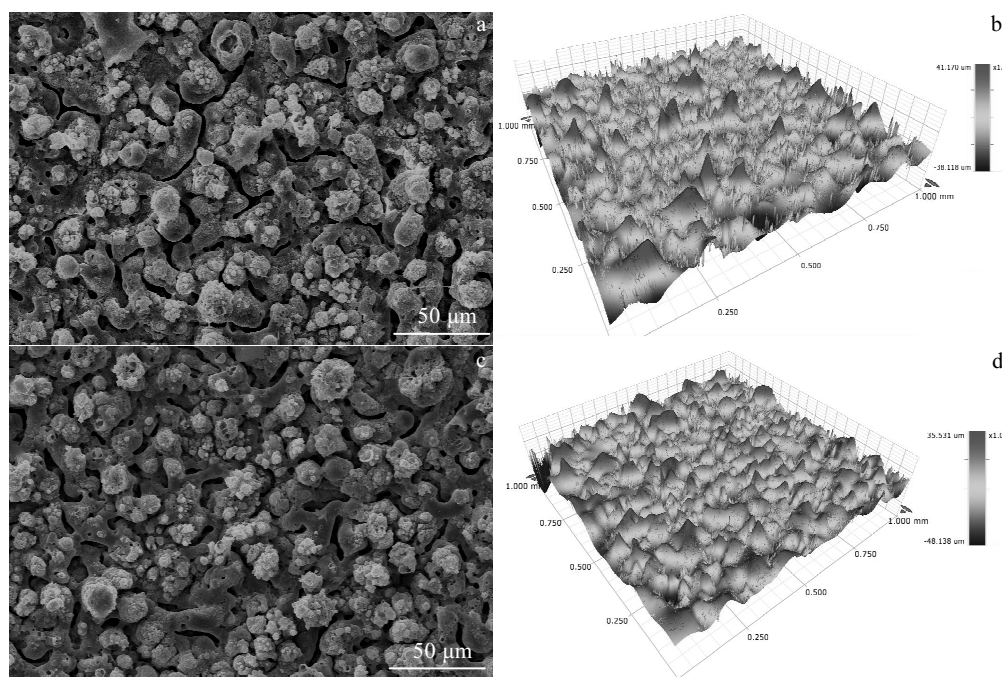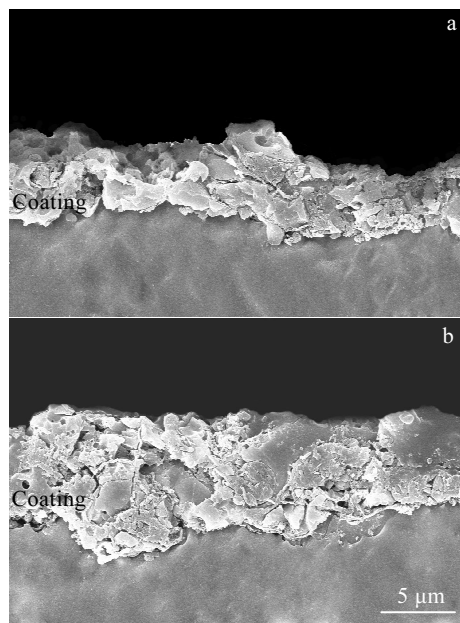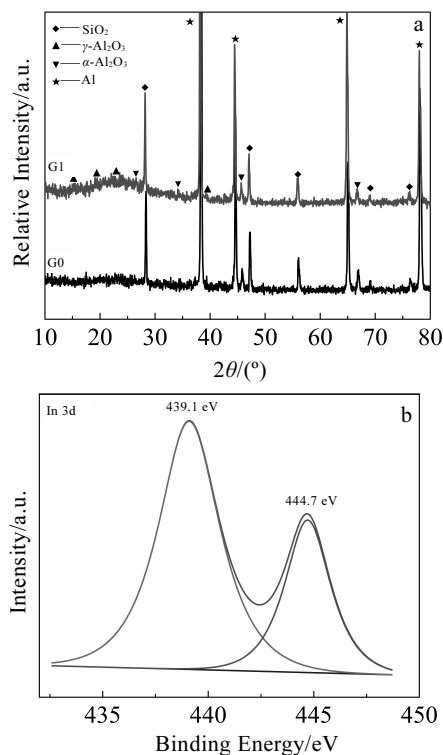

Fig.2   Surface morphologies of G0 (a), and G1 (c), and 3D topographies of G0 (b) and G1 (d)

**Table 1   Contents of In, Al, O and Si in the MAO coating (at%)**

Element	G0	G1
In	-	0.19
Al	25.13	20.73
O	41.50	43.56
Si	33.37	35.52

Fig.3   Cross-section morphologies of G0 (a) and G1 (b)

Fig.4   XRD patterns (a) and XPS spectrum (b) of the MAO

of SiO_2 came from the oxidation of Si in the substrate and the Na_2SiO_3 in the electrolyte. Due to local high temperature, amorphous Al_2O_3 will gradually transform to γ-Al_2O_3 and α-Al_2O_3[25].

According to the fitting result of XPS in Fig.4b, the In element existed in the micro-arc oxidation coating and the binding energy of 444.7 eV was a characteristic of the In_2O_3[26]. And In^{3+} reacted with OH^- in the electrolyte to form $In(OH)_3$. When the temperature reached 600 ℃, $In(OH)_3$ dehydrated completely to form In_2O_3. Through the analysis, the possible reactions during MAO process are as follows:

$$In^{3+}+3OH^- \xrightarrow{600\,℃} In(OH)_3 \qquad (1)$$

$$2In(OH)_3 \rightarrow In_2O_3+3H_2O \qquad (2)$$
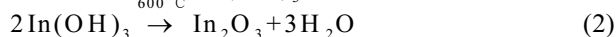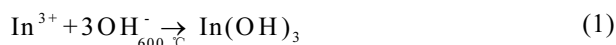
2.4   Thickness and the micro-hardness of the MAO coating

The thickness test results are shown in Fig.5a. The results indicated that the thickness of G0 was (5.2± 0.2) μm and that of G1 was (8.6±0.1) μm. That demonstrated the addition of In_2S_3 in the electrolyte resulted in the slight increase of the thickness of MAO coatings, which was consistent with the analysis in the voltage-time curves and cross-section morphologies.

Fig.5b shows the micro-hardness test results of substrate and MAO coatings G0 and G1. It can be seen from Fig. 5b that the micro-hardness of ZL108 alloy with the MAO coating was greater than that of the substrate, which was due to the formation of α-Al_2O_3, γ-Al_2O_3 and SiO_2 phases during the micro-arc oxidation process[27,28]. When In_2S_3 was added, the MAO coating became denser, so the micro-hardness of G1 was further improved compared with G0.
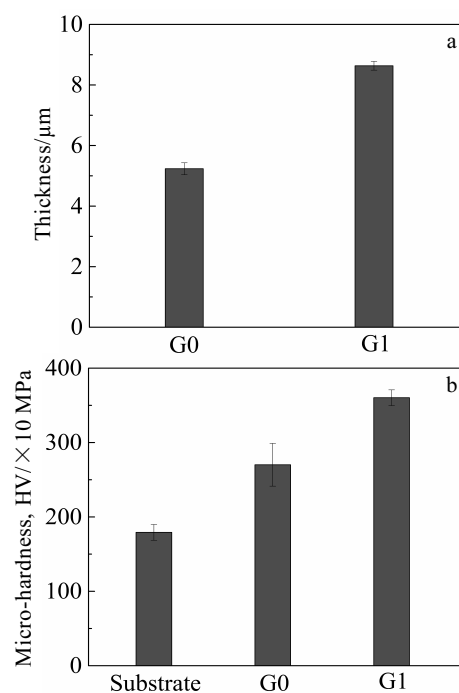
Fig.5   Thickness (a) and micro-hardness (b) of the MAO

2.5　Electrochemical measurements

Fig.6 shows the Nyquist plots and Bode plots of ZL108 alloy substrate and two MAO coatings (G0 and G1). It can be seen from Fig. 6a that in the Nyquist plots of G0 and G1 coatings, a high-frequency capacitor loop was followed by a low-frequency capacitor loop. The impedance semi-arc of the MAO coating was significantly enlarged compared with ZL108 alloy substrate. Moreover, the impedance semi-arc of G1 was bigger than that of G0. In the Nyquist plots, the radius of the arc tolerant resistance can reflect the corrosion rate of the samples. The larger the radius of the arc tolerant resistance, the smaller the corrosion rate, and the better the corrosion resistance of the samples[29,30]. This indicated that

the MAO coating G1 had better corrosion resistance than G0 and ZL108 alloy substrate. Through the observation and analysis of Bode curves in Fig. 6b and 6c, it can be found that the sample with the MAO coating had higher impedance value compared with the substrate. The impedance value was large, and the corrosion resistance of the samples was good. Especially after the addition of In_2S_3. The impedance value of G0: $R_1=1.496\times10^4$ $\Omega\cdot cm^2$, $R_2=2.87\times10^4$ $\Omega\cdot cm^2$; the impedance value of G1: $R_1=1.321\times10^5$ $\Omega\cdot cm^2$, $R_2=1.541\times10^5$ $\Omega\cdot cm^2$, as shown in Table 2. The reason for the above phenomenon and results was that the surface of G1 was denser than that of G0, which effectively prevented Cl^- from corroding the MAO coating.
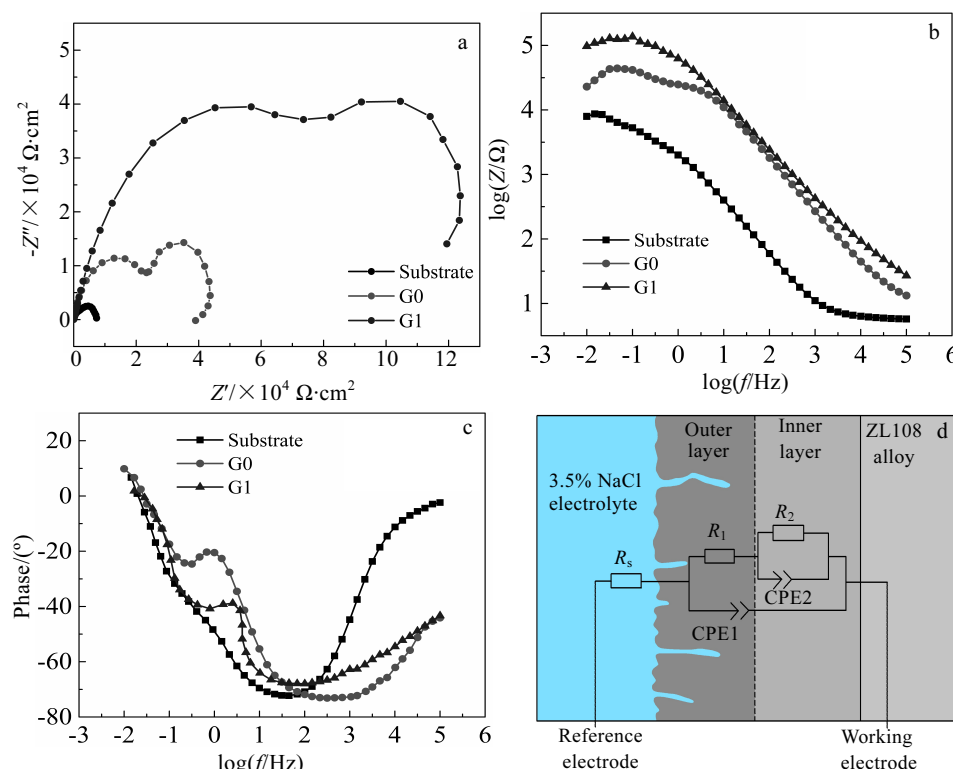

Fig.6　EIS spectra of the ZL108 alloy substrate and the two MAO-coated samples: (a) Nyquist plots, (b, c) Bode plots, and (d) equivalent circuit

The potentiodynamic polarization curve of MAO coatings and ZL108 alloy in 3.5 wt% NaCl solution is shown in Fig. 7. The corrosion potential (E_{coor}) and corrosion current density (i_{corr}) were directly derived from potentiodynamic polarization curves by Tafel region extrapolation and. The parameters obtained from the polarization curve are displayed in Table 3. It can be concluded from the data in the table that compared with ZL108 alloy substrate, MAO coatings (G0 and G1) had greater self-corrosion potential and lower self-corrosion current, and the corrosion rate of MAO coatings were smaller than that of the substrate through calculation, which indicated that MAO coatings had better corrosion resistance than ZL108 alloy substrate. In particular, the MAO coating G1 showed excellent corrosion resistance, which was consistent with previous EIS test results.
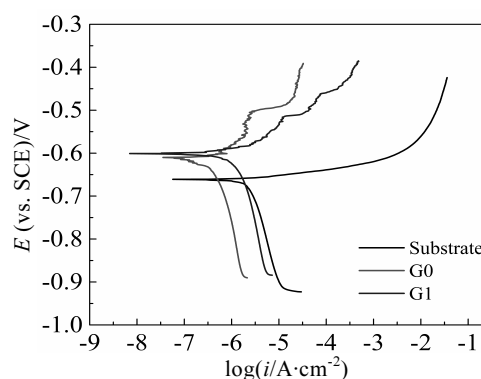

Fig.7　Polarization curves of the ZL108 alloy substrate and the two MAO-coated samples

Table 2   Electrochemical parameters obtained from EIS spectra of MAO coatings

Sample	$R_s/\Omega \cdot cm^2$	$CPE1/\Omega^{-1} \cdot cm^{-2} \cdot S^n$	n_1	$R_1/\Omega \cdot cm^2$	$CPE2/\Omega^{-1} \cdot cm^{-2} \cdot S^n$	n_2	$R_2/\Omega \cdot cm^2$
G0	8.629	2.685×10^{-6}	0.7842	1.496×10^4	5.352×10^{-5}	0.7615	2.857×10^4
G1	11.04	1.386×10^{-6}	0.8206	1.321×10^5	1.438×10^{-6}	0.8613	1.541×10^5

Table 3   Electrochemical data from the polarization tests for ZL108 alloy substrate and the two MAO-coated samples

Sample	E_{corr}/V	$i_{corr}/A \cdot cm^{-2}$	Corrosion rate/mm·a^{-1}
Substrate	-0.661	4.76×10^{-6}	1.60×10^{-1}
G0	-0.611	1.27×10^{-6}	4.29×10^{-2}
G1	-0.601	1.38×10^{-7}	4.67×10^{-3}

3   Conclusions

1) The addition of In_2S_3 can improve the micro-arc oxidation voltage and promote the micro-arc oxidation reaction of ZL108 aluminum alloy. The coating formation rate and the coating thickness were increased.

2) The addition of In_2S_3 increased the MAO coating thickness and micro-hardness. XRD analysis showed that γ-Al_2O_3, α-Al_2O_3 and SiO_2 were the main phases and the analysis of XPS spectrum proved that In_2O_3 existed on the MAO coating surface. SEM morphologies indicated that the surface and cross-section morphologies of the MAO coating became denser when In_2S_3 was added. And 3D topographies showed that the surface roughness was decreased.

3) The corrosion resistance of the coating sample was improved with the addition of In_2S_3. The impedance values of the outer layer and the inner layer of the MAO coating G0 in the EIS were 1.496×10^4 and 2.857×10^4 Ω/cm^2, and the impedance values of the outer layer and the inner layer of G1 in the EIS were 1.321×10^5 and 1.541×10^5 Ω/cm^2, respectively. The corrosion rate of the polarization curves of the substrate, the MAO coating without and with In_2S_3 were 1.6×10^{-1}, 4.29×10^{-2}, 4.67×10^{-3} mm/a, respectively.

References

1   Yang W, Xu D P, Guo Q Q *et al*. *Surface and Coatings Technology*[J], 2018, 349: 522

2   Garb C, Leitner M, Stauder B *et al*. *International Journal of Fatigue*[J], 2018, 111: 256

3   T O Mbuya, I Sinclair, A J Moffat *et al*. *International Journal of Fatigue*[J], 2012, 42: 227

4   Wang P, Gong Z Y, Hu J *et al*. *Surface Engineering*[J], 2019, 35: 627

5   Lim Tae Seop, Ryu Hyun Sam, Hong Seong-Hyeon. *Corrosion Science*[J], 2012, 62: 104

6   Wang P, Wu T, Xiao Y T *et al*. *Vacuum*[J], 2017, 142: 21

7   Xu J L, Liu F, Wang F P *et al*. *Journal of Alloys and Compounds*[J], 2009, 472(1-2): 276

8   LiH X, Song R G, Ji Z G. *Transactions of Nonferrous Metals Society of China*[J], 2013, 23(2): 406

9   Madhavi Y, Krishna L Rama, Narasaiah N. *International Journal of Fatigue*[J], 2019, 126: 297

10   Salih Durdu, Metin Usta. *Applied Surface Science*[J], 2012, 261: 774

11   Dou J H, Yu H J, Chen C Z. *Materials Letters*[J], 2019, 255: 126 578

12   Fazel M, Salimijazi H R, Golozar M A *et al*. *Applied Surface Science*[J], 2015, 324: 751

13   Bai L J, Dong B X, Chen G T *et al*. *Surface and Coatings Technology*[J], 2019, 374: 402

14   Luo H H, Cai Q Z, Wei B K *et al*. *Journal of Alloys and Compounds*[J], 2008, 464(1-2): 537

15   Feliu S, Llorente I. *Applied Surface Science*[J], 2015, 347: 736

16   Zeng R C, Zhang F, Lan Z D *et al*. *Corrosion Science*[J], 2014, 88: 452

17   Yan Y Y, Han Y, Li D C *et al*. *Applied Surface Science*[J], 2010, 256(21): 6359

18   Chen Q Z, Jiang Z Q, Tang S G *et al*. *Applied Surface Science*[J], 2017, 423: 939

19   Wang S Y, Si N C, Xia Y P *et al*. *Transactions of Nonferrous Metals Society of China*[J], 2015, 25(6): 1926

20   Metin Bedir, Mustafa Öztas. *Science in China Series E: Technological Sciences*[J], 2008, 51(5): 487

21   Chen F, Deng D, Lei Y L. *Journal of Nanoscience and Nanotechnology*[J], 2013, 13(10): 6928

22   Bouguila N, Kraini M, Najeh I *et al*. *Journal of Electronic Materials*[J], 2015, 44(11): 4213

23   Wang P, Wu T, Xiao Y T *et al*. *Materials Letters*[J], 2016, 182: 27

24   Sahand Sarbishei, Mohammad AliFaghihi Sani, Mohammad Reza Mohammadi. *Ceramics International*[J], 2016, 42(7): 8789

25   Wang P, Wu T, Xiao Y T *et al*. *Journal of Materials Engineering and Performance* [J], 2016, 25(9): 3972

26   Hellwig Malte, Parala Harish, Cybinksa Joanna *et al*. *Journal of Nanoscience and Nanotechnology*[J], 2011, 11(9): 8094

27   StudentM M, Dovhunyk V M, Klapkiv M D *et al*. *Materials Science*[J], 2012, 48(2): 180

28   Shi L, Sun C F, Gao P *et al*. *Applied Surface Science*[J], 2006, 252(10): 3591

29   Liu W Y, Liu Y, Lin Y H *et al*. *Applied Surface Science*[J], 2019, 475: 645

30   Wang P, Cao W J, Yang B *et al*. *International Journal of Applied Ceramic Technology*[J], 2019, 16: 2273

硫化铟对 ZL108 铝合金微弧氧化膜层结构和耐腐蚀性能的影响

王　平 [1,2,3]，胡　杰 [1]，李瑞阳 [1]，龚泽宇 [1]，刘济威 [1]，熊　丹 [1]，向　东 [1]，魏晓伟 [3]，祖小涛 [2]

(1. 西南石油大学 材料科学与工程学院，四川 成都 610500)

(2. 电子科技大学 物理学院，四川 成都 611731)

(3. 西华大学 材料科学与工程学院，四川 成都 610039)

摘　要： 在含有 In_2S_3 的硅酸盐电解液中对 ZL108 铝合金进行了微弧氧化处理。采用扫描电镜(SEM)、光学轮廓仪、X 射线衍射 (XRD)、X 射线光电子能谱（XPS）和电化学工作站等检测手段，研究了添加 In_2S_3 对 MAO 膜层微观结构、相组成和耐蚀性等的影响。结果表明，In_2S_3 的加入提高了微弧氧化电压，使膜层成膜速率增加，从而导致膜层厚度增加。在含有 In_2S_3 的电解液中形成的膜层致密性更好，膜层显微硬度提高，膜层的耐蚀性增强。膜层主要由 α-Al_2O_3、γ-Al_2O_3 和 SiO_2 相组成。XPS 检测结果表明 In_2S_3 在氧化过程中转变为 In_2O_3。因此，添加 In_2S_3 优化了 MAO 膜层结构，提高了 MAO 膜层的综合性能。

关键词： 微弧氧化；ZL108 铝合金；硫化铟；耐蚀性

作者简介：王 平，男，1981 年生，博士，教授，西南石油大学材料科学与工程学院，四川 成都 610500，电话：028-83037405，E-mail: 818wp@163.com